

Search for Supersymmetry with Gauge-Mediated Breaking in Diphoton Events with Missing Transverse Energy at CDF II

T. Aaltonen,²⁵ J. Adelman,¹⁵ B. Álvarez González,^{13,w} S. Amerio,^{46,45} D. Amidei,³⁶ A. Anastassov,⁴⁰ A. Annovi,²¹ J. Antos,¹⁶ G. Apollinari,¹⁹ A. Apresyan,⁵⁴ T. Arisawa,⁶⁵ A. Artikov,¹⁷ J. Asaadi,⁶⁰ W. Ashmanskas,¹⁹ A. Attal,⁴ A. Aurisano,⁶⁰ F. Azfar,⁴⁴ W. Badgett,¹⁹ A. Barbaro-Galtieri,³⁰ V. E. Barnes,⁵⁴ B. A. Barnett,²⁷ P. Barria,^{51,49} P. Bartos,¹⁶ G. Bauer,³⁴ P.-H. Beauchemin,³⁵ F. Bedeschi,⁴⁹ D. Beecher,³² S. Behari,²⁷ G. Bellettini,^{50,49} J. Bellinger,⁶⁷ D. Benjamin,¹⁸ A. Beretvas,¹⁹ A. Bhatti,⁵⁶ M. Binkley,¹⁹ D. Bisello,^{46,45} I. Bizjak,^{32,dd} R. E. Blair,² C. Blocker,⁸ B. Blumenfeld,²⁷ A. Bocci,¹⁸ A. Bodek,⁵⁵ V. Boisvert,⁵⁵ D. Bortoletto,⁵⁴ J. Boudreau,⁵³ A. Boveia,¹² B. Brau,^{12,b} A. Bridgeman,²⁶ L. Brigliadori,^{7,6} C. Bromberg,³⁷ E. Brubaker,¹⁵ J. Budagov,¹⁷ H. S. Budd,⁵⁵ S. Budd,²⁶ K. Burkett,¹⁹ G. Busetto,^{46,45} P. Bussey,²³ A. Buzatu,³⁵ K. L. Byrum,² S. Cabrera,^{18,y} C. Calancha,³³ S. Camarda,⁴ M. Campanelli,³⁷ M. Campbell,³⁶ F. Canelli,^{15,19} A. Canepa,⁴⁸ B. Carls,²⁶ D. Carlsmith,⁶⁷ R. Carosi,⁴⁹ S. Carrillo,^{20,o} S. Carron,¹⁹ B. Casal,¹³ M. Casarsa,¹⁹ A. Castro,^{7,6} P. Catastini,^{51,49} D. Cauz,⁶¹ V. Cavaliere,^{51,49} M. Cavalli-Sforza,⁴ A. Cerri,³⁰ L. Cerrito,^{32,r} S. H. Chang,²⁹ Y. C. Chen,¹ M. Chertok,⁹ G. Chiarelli,⁴⁹ G. Chlachidze,¹⁹ F. Chlebana,¹⁹ K. Cho,²⁹ D. Chokheli,¹⁷ J. P. Chou,²⁴ G. Choudalakis,³⁴ K. Chung,^{19,p} W. H. Chung,⁶⁷ Y. S. Chung,⁵⁵ T. Chwalek,²⁸ C. I. Ciobanu,⁴⁷ M. A. Ciocci,^{51,49} A. Clark,²² D. Clark,⁸ G. Compostella,⁴⁵ M. E. Convery,¹⁹ J. Conway,⁹ M. Corbo,⁴⁷ M. Cordelli,²¹ C. A. Cox,⁹ D. J. Cox,⁹ F. Crescioli,^{50,49} C. Cuenca Almenar,⁶⁸ J. Cuevas,^{13,w} R. Culbertson,¹⁹ J. C. Cully,³⁶ D. Dagenhart,¹⁹ M. Datta,¹⁹ T. Davies,²³ P. de Barbaro,⁵⁵ S. De Cecco,⁵⁷ A. Deisher,³⁰ G. De Lorenzo,⁴ M. Dell'Orso,^{50,49} C. Deluca,⁴ L. Demortier,⁵⁶ J. Deng,^{18,g} M. Deninno,⁶ M. d'Errico,^{46,45} A. Di Canto,^{50,49} G. P. di Giovanni,⁴⁷ B. Di Ruzza,⁴⁹ J. R. Dittmann,⁵ M. D'Onofrio,⁴ S. Donati,^{50,49} P. Dong,¹⁹ T. Dorigo,⁴⁵ S. Dube,⁵⁹ K. Ebina,⁶⁵ A. Elagin,⁶⁰ R. Erbacher,⁹ D. Errede,²⁶ S. Errede,²⁶ N. Ershaidat,^{47,cc} R. Eusebi,⁶⁰ H. C. Fang,³⁰ S. Farrington,⁴⁴ W. T. Fedorko,¹⁵ R. G. Feild,⁶⁸ M. Feindt,²⁸ J. P. Fernandez,³³ C. Ferrazza,^{52,49} R. Field,²⁰ G. Flanagan,^{54,t} R. Forrest,⁹ M. J. Frank,⁵ M. Franklin,²⁴ J. C. Freeman,¹⁹ I. Furic,²⁰ M. Gallinaro,⁵⁶ J. Galyardt,¹⁴ F. Garberon,¹² J. E. Garcia,²² A. F. Garfinkel,⁵⁴ P. Garosi,^{51,49} K. Genser,¹⁹ H. Gerberich,²⁶ D. Gerdes,³⁶ A. Gessler,²⁸ S. Giagu,^{58,57} V. Giakoumopoulou,³ P. Giannetti,⁴⁹ K. Gibson,⁵³ J. L. Gimmell,⁵⁵ C. M. Ginsburg,¹⁹ N. Giokaris,³ M. Giordani,^{62,61} P. Giromini,²¹ M. Giunta,⁴⁹ G. Giurgiu,²⁷ V. Glagolev,¹⁷ D. Glenzinski,¹⁹ M. Gold,³⁹ N. Goldschmidt,²⁰ A. Golossanov,¹⁹ G. Gomez,¹³ G. Gomez-Ceballos,³⁴ M. Goncharov,³⁴ O. González,³³ I. Gorelov,³⁹ A. T. Goshaw,¹⁸ K. Goulianos,⁵⁶ A. Gresele,^{46,45} S. Grinstein,⁴ C. Grosso-Pilcher,¹⁵ R. C. Group,¹⁹ U. Grundler,²⁶ J. Guimaraes da Costa,²⁴ Z. Gunay-Unalan,³⁷ C. Haber,³⁰ K. Hahn,³⁴ S. R. Hahn,¹⁹ E. Halkiadakis,⁵⁹ B.-Y. Han,⁵⁵ J. Y. Han,⁵⁵ F. Happacher,²¹ K. Hara,⁶³ D. Hare,⁵⁹ M. Hare,⁶⁴ R. F. Harr,⁶⁶ M. Hartz,⁵³ K. Hatakeyama,⁵ C. Hays,⁴⁴ M. Heck,²⁸ J. Heinrich,⁴⁸ C. Henderson,³⁴ M. Herndon,⁶⁷ J. Heuser,²⁸ S. Hewamanage,⁵ D. Hidas,⁵⁹ C. S. Hill,^{12,d} D. Hirschbuehl,²⁸ A. Hocker,¹⁹ S. Hou,¹ M. Houlden,³¹ S.-C. Hsu,³⁰ B. T. Huffman,⁴⁴ R. E. Hughes,⁴¹ M. Hurwitz,¹⁵ U. Husemann,⁶⁸ M. Hussein,³⁷ J. Huston,³⁷ J. Incandela,¹² G. Introzzi,⁴⁹ M. Iori,^{58,57} A. Ivanov,^{9,q} E. James,¹⁹ D. Jang,¹⁴ B. Jayatilaka,¹⁸ E. J. Jeon,²⁹ M. K. Jha,⁶ S. Jindariani,¹⁹ W. Johnson,⁹ M. Jones,⁵⁴ K. K. Joo,²⁹ S. Y. Jun,¹⁴ J. E. Jung,²⁹ T. R. Junk,¹⁹ T. Kamon,⁶⁰ D. Kar,²⁰ P. E. Karchin,⁶⁶ Y. Kato,^{43,n} R. Kephart,¹⁹ W. Ketchum,¹⁵ J. Keung,⁴⁸ V. Khotilovich,⁶⁰ B. Kilminster,¹⁹ D. H. Kim,²⁹ H. S. Kim,²⁹ H. W. Kim,²⁹ J. E. Kim,²⁹ M. J. Kim,²¹ S. B. Kim,²⁹ S. H. Kim,⁶³ Y. K. Kim,¹⁵ N. Kimura,⁶⁵ L. Kirsch,⁸ S. Klimentenko,²⁰ B. Knuteson,³⁴ K. Kondo,⁶⁵ D. J. Kong,²⁹ J. Konigsberg,²⁰ A. Korytov,²⁰ A. V. Kotwal,¹⁸ M. Kreps,²⁸ J. Kroll,⁴⁸ D. Krop,¹⁵ N. Krumnack,⁵ M. Kruse,¹⁸ V. Krutelyov,¹² T. Kuhr,²⁸ N. P. Kulkarni,⁶⁶ M. Kurata,⁶³ S. Kwang,¹⁵ A. T. Laasanen,⁵⁴ S. Lami,⁴⁹ S. Lammel,¹⁹ M. Lancaster,³² R. L. Lander,⁹ K. Lannon,^{41,v} A. Lath,⁵⁹ G. Latino,^{51,49} I. Lazzizzera,^{46,45} T. LeCompte,² E. Lee,⁶⁰ H. S. Lee,¹⁵ J. S. Lee,²⁹ S. W. Lee,^{60,x} S. Leone,⁴⁹ J. D. Lewis,¹⁹ C.-J. Lin,³⁰ J. Linacre,⁴⁴ M. Lindgren,¹⁹ E. Lipeles,⁴⁸ A. Lister,²² D. O. Litvintsev,¹⁹ C. Liu,⁵³ T. Liu,¹⁹ N. S. Lockyer,⁴⁸ A. Loginov,⁶⁸ L. Lovas,¹⁶ D. Lucchesi,^{46,45} J. Lueck,²⁸ P. Lujan,³⁰ P. Lukens,¹⁹ G. Lungu,⁵⁶ J. Lys,³⁰ R. Lysak,¹⁶ D. MacQueen,³⁵ R. Madrak,¹⁹ K. Maeshima,¹⁹ K. Makhoul,³⁴ P. Maksimovic,²⁷ S. Malde,⁴⁴ S. Malik,³² G. Manca,^{31,f} A. Manousakis-Katsikakis,³ F. Margaroli,⁵⁴ C. Marino,²⁸ C. P. Marino,²⁶ A. Martin,⁶⁸ V. Martin,^{23,1} M. Martínez,⁴ R. Martínez-Ballarín,³³ P. Mastrandrea,⁵⁷ M. Mathis,²⁷ M. E. Mattson,⁶⁶ P. Mazzanti,⁶ K. S. McFarland,⁵⁵ P. McIntyre,⁶⁰ R. McNulty,^{31,k} A. Mehta,³¹ P. Mehtala,²⁵ A. Menzione,⁴⁹ C. Mesropian,⁵⁶ T. Miao,¹⁹ D. Miettlicki,³⁶ N. Miladinovic,⁸ R. Miller,³⁷ C. Mills,²⁴ M. Milnik,²⁸ A. Mitra,¹ G. Mitselmakher,²⁰ H. Miyake,⁶³ S. Moed,²⁴ N. Moggi,⁶ M. N. Mondragon,^{19,o} C. S. Moon,²⁹ R. Moore,¹⁹ M. J. Morello,⁴⁹ J. Morlock,²⁸ P. Movilla Fernandez,¹⁹ J. Mülmenstädt,³⁰ A. Mukherjee,¹⁹ Th. Muller,²⁸ P. Murat,¹⁹ M. Mussini,^{7,6} J. Nachtman,^{19,p} Y. Nagai,⁶³ J. Naganoma,⁶³ K. Nakamura,⁶³ I. Nakano,⁴² A. Napier,⁶⁴ J. Nett,⁶⁷ C. Neu,^{48,aa} M. S. Neubauer,²⁶ S. Neubauer,²⁸ J. Nielsen,^{30,h} L. Nodulman,² M. Norman,¹¹ O. Norniella,²⁶ E. Nurse,³²

L. Oakes,⁴⁴ S. H. Oh,¹⁸ Y. D. Oh,²⁹ I. Oksuzian,²⁰ T. Okusawa,⁴³ R. Orava,²⁵ K. Osterberg,²⁵ S. Pagan Griso,^{46,45} C. Pagliarone,⁶¹ E. Palencia,¹⁹ V. Papadimitriou,¹⁹ A. Papaikonomou,²⁸ A. A. Paramanov,² B. Parks,⁴¹ S. Pashapour,³⁵ J. Patrick,¹⁹ G. Pauletta,^{62,61} M. Paulini,¹⁴ C. Paus,³⁴ T. Peiffer,²⁸ D. E. Pellett,⁹ A. Penzo,⁶¹ T. J. Phillips,¹⁸ G. Piacentino,⁴⁹ E. Pianori,⁴⁸ L. Pinera,²⁰ K. Pitts,²⁶ C. Plager,¹⁰ L. Pondrom,⁶⁷ K. Potamianos,⁵⁴ O. Poukhov,^{17,a} F. Prokoshin,^{17,z} A. Pronko,¹⁹ F. Ptohos,^{19,j} E. Pueschel,¹⁴ G. Punzi,^{50,49} J. Pursley,⁶⁷ J. Rademacker,^{44,d} A. Rahaman,⁵³ V. Ramakrishnan,⁶⁷ N. Ranjan,⁵⁴ I. Redondo,³³ P. Renton,⁴⁴ M. Renz,²⁸ M. Rescigno,⁵⁷ S. Richter,²⁸ F. Rimondi,^{7,6} L. Ristori,⁴⁹ A. Robson,²³ T. Rodrigo,¹³ T. Rodriguez,⁴⁸ E. Rogers,²⁶ S. Rolli,⁶⁴ R. Roser,¹⁹ M. Rossi,⁶¹ R. Rossin,¹² P. Roy,³⁵ A. Ruiz,¹³ J. Russ,¹⁴ V. Rusu,¹⁹ B. Rutherford,¹⁹ H. Saarikko,²⁵ A. Safonov,⁶⁰ W. K. Sakumoto,⁵⁵ L. Santi,^{62,61} L. Sartori,⁴⁹ K. Sato,⁶³ A. Savoy-Navarro,⁴⁷ P. Schlabach,¹⁹ A. Schmidt,²⁸ E. E. Schmidt,¹⁹ M. A. Schmidt,¹⁵ M. P. Schmidt,^{68,a} M. Schmitt,⁴⁰ T. Schwarz,⁹ L. Scodellaro,¹³ A. Scribano,^{51,49} F. Scuri,⁴⁹ A. Sedov,⁵⁴ S. Seidel,³⁹ Y. Seiya,⁴³ A. Semenov,¹⁷ L. Sexton-Kennedy,¹⁹ F. Sforza,^{50,49} A. Sfyrla,²⁶ S. Z. Shalhout,⁶⁶ T. Shears,³¹ P. F. Shepard,⁵³ M. Shimojima,^{63,u} S. Shiraishi,¹⁵ M. Shochet,¹⁵ Y. Shon,⁶⁷ I. Shreyber,³⁸ A. Simonenko,¹⁷ P. Sinervo,³⁵ A. Sisakyan,¹⁷ A. J. Slaughter,¹⁹ J. Slaunwhite,⁴¹ K. Sliwa,⁶⁴ J. R. Smith,⁹ F. D. Snider,¹⁹ R. Snihur,³⁵ A. Soha,¹⁹ S. Somalwar,⁵⁹ V. Sorin,⁴ T. Spreitzer,³⁵ P. Squillacioti,^{51,49} M. Stanitzki,⁶⁸ R. St. Denis,²³ B. Stelzer,³⁵ O. Stelzer-Chilton,³⁵ D. Stentz,⁴⁰ J. Strogas,³⁹ G. L. Strycker,³⁶ J. S. Suh,²⁹ A. Sukhanov,²⁰ I. Suslov,¹⁷ A. Taffard,^{26,g} R. Takashima,⁴² Y. Takeuchi,⁶³ R. Tanaka,⁴² J. Tang,¹⁵ M. Tecchio,³⁶ P. K. Teng,¹ J. Thom,^{19,i} J. Thome,¹⁴ G. A. Thompson,²⁶ E. Thomson,⁴⁸ P. Tipton,⁶⁸ P. Tito-Guzmán,³³ S. Tkaczyk,¹⁹ D. Toback,⁶⁰ S. Tokar,¹⁶ K. Tollefson,³⁷ T. Tomura,⁶³ D. Tonelli,¹⁹ S. Torre,²¹ D. Torretta,¹⁹ P. Totaro,^{62,61} S. Tourneur,⁴⁷ M. Trovato,^{52,49} S.-Y. Tsai,¹ Y. Tu,⁴⁸ N. Turini,^{51,50} F. Ukegawa,⁶³ S. Uozumi,²⁹ N. van Remortel,^{25,c} A. Varganov,³⁶ E. Vataga,^{52,49} F. Vázquez,^{20,o} G. Velev,¹⁹ C. Vellidis,³ M. Vidal,³³ I. Vila,¹³ R. Vilar,¹³ M. Vogel,³⁹ I. Volobouev,^{30,x} G. Volpi,^{50,49} P. Wagner,⁴⁸ R. G. Wagner,² R. L. Wagner,¹⁹ W. Wagner,^{28,bb} J. Wagner-Kuhr,²⁸ T. Wakisaka,⁴³ R. Wallny,¹⁰ S. M. Wang,¹ A. Warburton,³⁵ D. Waters,³² M. Weinberger,⁶⁰ J. Weinelt,²⁸ W. C. Wester III,¹⁹ B. Whitehouse,⁶⁴ D. Whiteson,^{48,g} A. B. Wicklund,² E. Wicklund,¹⁹ S. Wilbur,¹⁵ G. Williams,³⁵ H. H. Williams,⁴⁸ P. Wilson,¹⁹ B. L. Winer,⁴¹ P. Wittich,^{19,i} S. Wolbers,¹⁹ C. Wolfe,¹⁵ H. Wolfe,⁴¹ T. Wright,³⁶ X. Wu,²² F. Würthwein,¹¹ S. Xie,³⁴ A. Yagil,¹¹ K. Yamamoto,⁴³ J. Yamaoka,¹⁸ U. K. Yang,^{15,s} Y. C. Yang,²⁹ W. M. Yao,³⁰ G. P. Yeh,¹⁹ K. Yi,^{19,p} J. Yoh,¹⁹ K. Yorita,⁶⁵ T. Yoshida,^{43,m} G. B. Yu,¹⁸ I. Yu,²⁹ S. S. Yu,¹⁹ J. C. Yun,¹⁹ A. Zanetti,⁶¹ Y. Zeng,¹⁸ X. Zhang,²⁶ Y. Zheng,^{10,e} and S. Zucchelli^{7,6}

¹*Institute of Physics, Academia Sinica, Taipei, Taiwan 11529, Republic of China*

²*Argonne National Laboratory, Argonne, Illinois 60439, USA*

³*University of Athens, 157 71 Athens, Greece*

⁴*Institut de Física d'Altes Energies, Universitat Autònoma de Barcelona, E-08193, Bellaterra (Barcelona), Spain*

⁵*Baylor University, Waco, Texas 76798, USA*

⁶*Istituto Nazionale di Fisica Nucleare Bologna, I-40127 Bologna, Italy*

⁷*University of Bologna, I-40127 Bologna, Italy*

⁸*Brandeis University, Waltham, Massachusetts 02254, USA*

⁹*University of California, Davis, Davis, California 95616, USA*

¹⁰*University of California, Los Angeles, Los Angeles, California 90024, USA*

¹¹*University of California, San Diego, La Jolla, California 92093, USA*

¹²*University of California, Santa Barbara, Santa Barbara, California 93106, USA*

¹³*Instituto de Física de Cantabria, CSIC-University of Cantabria, 39005 Santander, Spain*

¹⁴*Carnegie Mellon University, Pittsburgh, Pennsylvania 15213, USA*

¹⁵*Enrico Fermi Institute, University of Chicago, Chicago, Illinois 60637, USA*

¹⁶*Comenius University, 842 48 Bratislava, Slovakia; Institute of Experimental Physics, 040 01 Kosice, Slovakia*

¹⁷*Joint Institute for Nuclear Research, RU-141980 Dubna, Russia*

¹⁸*Duke University, Durham, North Carolina 27708, USA*

¹⁹*Fermi National Accelerator Laboratory, Batavia, Illinois 60510, USA*

²⁰*University of Florida, Gainesville, Florida 32611, USA*

²¹*Laboratori Nazionali di Frascati, Istituto Nazionale di Fisica Nucleare, I-00044 Frascati, Italy*

²²*University of Geneva, CH-1211 Geneva 4, Switzerland*

²³*Glasgow University, Glasgow G12 8QQ, United Kingdom*

²⁴*Harvard University, Cambridge, Massachusetts 02138, USA*

²⁵*Division of High Energy Physics, Department of Physics, University of Helsinki and Helsinki Institute of Physics, FIN-00014, Helsinki, Finland*

²⁶*University of Illinois, Urbana, Illinois 61801, USA*

²⁷*The Johns Hopkins University, Baltimore, Maryland 21218, USA*

²⁸*Institut für Experimentelle Kernphysik, Karlsruhe Institute of Technology, D-76131 Karlsruhe, Germany*

- ²⁹*Center for High Energy Physics: Kyungpook National University, Daegu 702-701, Korea;*
Seoul National University, Seoul 151-742, Korea;
Sungkyunkwan University, Suwon 440-746, Korea;
Korea Institute of Science and Technology Information, Daejeon 305-806, Korea;
Chonnam National University, Gwangju 500-757, Korea;
Chonbuk National University, Jeonju 561-756, Korea
- ³⁰*Ernest Orlando Lawrence Berkeley National Laboratory, Berkeley, California 94720, USA*
- ³¹*University of Liverpool, Liverpool L69 7ZE, United Kingdom*
- ³²*University College London, London WC1E 6BT, United Kingdom*
- ³³*Centro de Investigaciones Energeticas Medioambientales y Tecnologicas, E-28040 Madrid, Spain*
- ³⁴*Massachusetts Institute of Technology, Cambridge, Massachusetts 02139, USA*
- ³⁵*Institute of Particle Physics: McGill University, Montréal, Québec, Canada H3A 2T8;*
Simon Fraser University, Burnaby, British Columbia, Canada V5A 1S6;
University of Toronto, Toronto, Ontario, Canada M5S 1A7;
and TRIUMF, Vancouver, British Columbia, Canada V6T 2A3
- ³⁶*University of Michigan, Ann Arbor, Michigan 48109, USA*
- ³⁷*Michigan State University, East Lansing, Michigan 48824, USA*
- ³⁸*Institution for Theoretical and Experimental Physics, ITEP, Moscow 117259, Russia*
- ³⁹*University of New Mexico, Albuquerque, New Mexico 87131, USA*
- ⁴⁰*Northwestern University, Evanston, Illinois 60208, USA*
- ⁴¹*The Ohio State University, Columbus, Ohio 43210, USA*
- ⁴²*Okayama University, Okayama 700-8530, Japan*
- ⁴³*Osaka City University, Osaka 588, Japan*
- ⁴⁴*University of Oxford, Oxford OX1 3RH, United Kingdom*
- ⁴⁵*Istituto Nazionale di Fisica Nucleare, Sezione di Padova-Trento, I-35131 Padova, Italy*
- ⁴⁶*University of Padova, I-35131 Padova, Italy*
- ⁴⁷*LPNHE, Universite Pierre et Marie Curie/IN2P3-CNRS, UMR7585, Paris, F-75252 France*
- ⁴⁸*University of Pennsylvania, Philadelphia, Pennsylvania 19104, USA*
- ⁴⁹*Istituto Nazionale di Fisica Nucleare Pisa, I-56127 Pisa, Italy*
- ⁵⁰*University of Pisa, I-56127 Pisa, Italy*
- ⁵¹*University of Siena, I-56127 Pisa, Italy*
- ⁵²*Scuola Normale Superiore, I-56127 Pisa, Italy*
- ⁵³*University of Pittsburgh, Pittsburgh, Pennsylvania 15260, USA*
- ⁵⁴*Purdue University, West Lafayette, Indiana 47907, USA*
- ⁵⁵*University of Rochester, Rochester, New York 14627, USA*
- ⁵⁶*The Rockefeller University, New York, New York 10021, USA*
- ⁵⁷*Istituto Nazionale di Fisica Nucleare, Sezione di Roma 1, I-00185 Roma, Italy*
- ⁵⁸*Sapienza Università di Roma, I-00185 Roma, Italy*
- ⁵⁹*Rutgers University, Piscataway, New Jersey 08855, USA*
- ⁶⁰*Texas A&M University, College Station, Texas 77843, USA*
- ⁶¹*Istituto Nazionale di Fisica Nucleare Trieste/Udine, I-34100 Trieste, I-33100 Udine, Italy*
- ⁶²*University of Trieste/Udine, I-33100 Udine, Italy*
- ⁶³*University of Tsukuba, Tsukuba, Ibaraki 305, Japan*
- ⁶⁴*Tufts University, Medford, Massachusetts 02155, USA*
- ⁶⁵*Waseda University, Tokyo 169, Japan*
- ⁶⁶*Wayne State University, Detroit, Michigan 48201, USA*
- ⁶⁷*University of Wisconsin, Madison, Wisconsin 53706, USA*
- ⁶⁸*Yale University, New Haven, Connecticut 06520, USA*
- (Received 19 October 2009; published 4 January 2010)

We present the results of a search for supersymmetry with gauge-mediated breaking and $\tilde{\chi}_1^0 \rightarrow \gamma\tilde{G}$ in the $\gamma\gamma +$ missing transverse energy final state. In $2.6 \pm 0.2 \text{ fb}^{-1}$ of $p\bar{p}$ collisions at $\sqrt{s} = 1.96 \text{ TeV}$ recorded by the CDF II detector we observe no candidate events, consistent with a standard model background expectation of 1.4 ± 0.4 events. We set limits on the cross section at the 95% C.L. and place the world's best limit of $149 \text{ GeV}/c^2$ on the $\tilde{\chi}_1^0$ mass at $\tau_{\tilde{\chi}_1^0} \ll 1 \text{ ns}$. We also exclude regions in the $\tilde{\chi}_1^0$ mass-lifetime plane for $\tau_{\tilde{\chi}_1^0} \lesssim 2 \text{ ns}$.

The standard model (SM) of elementary particles has been enormously successful, but is incomplete. Theoretical motivations [1] and the observation of the “ $ee\gamma\gamma + \text{missing transverse energy} (\cancel{E}_T)$ ” [2,3] candidate event by the CDF experiment during Run I at the Fermilab Tevatron provide a compelling rationale to search for the production and decay of new heavy particles that produce events with final state photons and \cancel{E}_T in collider experiments. Of particular theoretical interest are supersymmetry (SUSY) models with gauge-mediated SUSY-breaking (GMSB) [1]. These models solve the “naturalness problem” [4] and provide a low-mass dark matter candidate that is both consistent with inflation and astronomical observations [5]. Since many versions of these models have a similar phenomenology, we consider a scenario in which the lightest neutralino ($\tilde{\chi}_1^0$) decays almost exclusively ($> 96\%$) into a photon (γ) and a weakly interacting, stable gravitino (\tilde{G}). The \tilde{G} gives rise to \cancel{E}_T by leaving the detector without depositing any energy [6]. In these models, the $\tilde{\chi}_1^0$ is favored to have a lifetime on the order of a nanosecond, and the \tilde{G} is a warm dark matter candidate with a mass in the range $0.5 < m_{\tilde{G}} < 1.5 \text{ keV}/c^2$ [7]. Other direct searches [8–10] have constrained the mass of the $\tilde{\chi}_1^0$ to be greater than $100 \text{ GeV}/c^2$ for various points in parameter space. At the Tevatron sparticle production is predicted to result primarily in gaugino pairs, and the $\tilde{\chi}_1^0$ mass ($m_{\tilde{\chi}_1^0}$) and lifetime ($\tau_{\tilde{\chi}_1^0}$) are the two most important parameters in determining the final states and their kinematics [1]. Different search strategies are required for $\tilde{\chi}_1^0$ lifetimes above and below about a nanosecond [11].

This Letter describes a search for GMSB in which gaugino pairs are directly produced and quickly decay to the $\gamma\gamma + \cancel{E}_T + X$ final state, where X denotes other high- E_T final state particles [12]. We use a data set corresponding to an integrated luminosity of $2.6 \pm 0.2 \text{ fb}^{-1}$ of $p\bar{p}$ collisions collected with the CDF II detector [13] at $\sqrt{s} = 1.96 \text{ TeV}$. This data set is 10 times larger than the one used in our previous search [8]. For the first time in this channel we use a new photon timing system [14] and a new model of the \cancel{E}_T resolution (METMODEL) [15]. These additions significantly improve our rejection of backgrounds from instrumental and noncollision sources, which allows us to considerably enhance the sensitivity of the search for large $\tilde{\chi}_1^0$ masses compared to other Tevatron searches [9]. We also extend the search by addressing $\tilde{\chi}_1^0$ lifetimes up to 2 ns, which are favored for larger $m_{\tilde{\chi}_1^0}$.

Here we briefly describe the aspects of the detector [13] relevant to this analysis. The magnetic spectrometer consists of tracking devices that measure the z position and time of the $p\bar{p}$ interaction, and the momenta of charged particles inside a superconducting solenoid magnet. The calorimeter consists of electromagnetic (EM) and hadronic (HAD) compartments and is divided into a central part that surrounds the solenoid coil ($|\eta| < 1.1$) [2] and a pair of end plugs that cover the region $1.1 < |\eta| < 3.6$. The cal-

orimeters are used to identify and measure the four-momenta of photons, electrons, and jets (j) [16] and to provide \cancel{E}_T information. The EM calorimeter is instrumented with a timing system (EMTiming) [14] that measures the arrival time of photons.

Our analysis begins with diphoton events passing the CDF three-level trigger. The combined trigger selection efficiency is effectively 100% if both photons have $|\eta| < 1.1$ and $E_T > 13 \text{ GeV}$ [12,15]. Offline, both photons are required to be in the fiducial part of the calorimeter and to pass the standard CDF photon identification and isolation requirements [8], with two minor modifications to remove instrumental and electron backgrounds [15,17]. The remaining events are dominated by SM production of $\gamma\gamma$, γj with $j \rightarrow \gamma_{\text{fake}}$, and $jj \rightarrow \gamma_{\text{fake}}\gamma_{\text{fake}}$, where γ_{fake} is any object misidentified as a photon. To minimize the number of these events with large \cancel{E}_T due to calorimeter energy mismeasurements, we remove events where the azimuthal angle between the \cancel{E}_T and the second-highest E_T photon is $|\Delta\phi| < 0.3$ or if any jet points to an uninstrumented region of the calorimeter [15]. We require a primary collision vertex position with $|z_{\text{vertex}}| < 60 \text{ cm}$ in order to reduce noncollision backgrounds and to maintain the projective nature of the photon reconstruction in the calorimeter. For events with multiple reconstructed vertices we recalculate the E_T of both photons and \cancel{E}_T values if picking a different vertex for them reduces the event \cancel{E}_T .

Noncollision backgrounds coming from cosmic rays and beam-related effects can produce $\gamma\gamma + \cancel{E}_T$ candidates, and are removed from the inclusive $\gamma\gamma$ sample using a number of techniques. Photon candidates from cosmic rays are not correlated in time with collisions. Therefore, events are removed if the timing of either photon, corrected for average path length (t_γ), indicates a noncollision source [15,17]. Photon candidates can also be produced by beam-related muons that originate upstream of the detector (from the more intense p beam). These are suppressed using standard beam halo identification requirements [17]. A total of 38 053 inclusive $\gamma\gamma$ candidate events pass all the selection requirements.

Backgrounds to the $\gamma\gamma + \cancel{E}_T$ final state from SM $\gamma\gamma$, $\gamma\gamma_{\text{fake}}$, $\gamma_{\text{fake}}\gamma_{\text{fake}}$, and fake \cancel{E}_T arise due to energy mismeasurements in the calorimeter or to event reconstruction pathologies. We use the METMODEL [15] to select events with real and significant \cancel{E}_T , as part of the optimization, and to predict the contribution of SM backgrounds with fake \cancel{E}_T due to normal energy measurement fluctuations. This algorithm considers the clustered (jets) and unclustered energy in the event and calculates the probability for fluctuations in the energy measurement to produce $\cancel{E}_T^{\text{fluct}}$ equivalent to or larger than the measured \cancel{E}_T , $P_{\cancel{E}_T^{\text{fluct}} \geq \cancel{E}_T}$. This probability is then used to define a \cancel{E}_T significance as $-\log_{10}(P_{\cancel{E}_T^{\text{fluct}} \geq \cancel{E}_T})$. Events with true and fake \cancel{E}_T of the same value have, on average, different \cancel{E}_T significance. We use pseudoexperiments to estimate the expected

\cancel{E}_T -significance distribution for SM events with fake \cancel{E}_T , and the number of mismeasured events above a given \cancel{E}_T -significance requirement. The jets and unclustered energy are smeared according to their resolution functions in the event. The systematic uncertainty in the METMODEL is dominated by the uncertainty in the resolution functions.

The METMODEL does not account for reconstruction pathologies in SM events without intrinsic \cancel{E}_T , such as a wrong choice of the primary interaction vertex or triphoton events with a lost photon. To obtain the prediction for this background we model SM kinematics and event reconstruction using a $\gamma\gamma$ sample generated with a PYTHIA Monte Carlo (MC) [18] that incorporates a detector simulation [19]. Since the pathologies from γj and jj sources are similar in nature, but not included directly in the simulation, we normalize the sample to the number of events in the inclusive $\gamma\gamma$ data sample. We subtract the expectations for energy mismeasurement fluctuations in the MC to avoid double counting. Uncertainties are dominated by the statistics of the MC sample, but also include the small differences between the measured response of the METMODEL to MC simulation events and real data.

Electroweak production of W and Z bosons which decay to leptons can also produce the $\gamma\gamma + \cancel{E}_T$ signature where one or more of the photons can be fake, but the \cancel{E}_T is due to one or more neutrinos. To estimate the contribution from these backgrounds we use MC simulations normalized to their theoretical cross sections, taking into account all the leptonic decay modes. The Baur MC [20] is used to simulate $W\gamma$ and $Z\gamma$ production and decay where initial and final state radiation (ISR and FSR) produce W or $Z + \gamma\gamma$ events. The PYTHIA MC is used to simulate backgrounds

where both photons are fakes: namely, W and Z , with photons from ISR and FSR removed, and $t\bar{t}$ sources. To minimize the dependence of our predictions on potential “MC-data” differences we scale our MC predictions to the observed number of $e\gamma$ events [15] in data where we use the same diphoton triggers and analysis selection procedures used to select the inclusive $\gamma\gamma$ sample. Uncertainties are dominated by the statistics of the MC and $e\gamma$ normalization data sample.

Noncollision backgrounds are estimated using the data. We identify a cosmic-enhanced sample by using the selected inclusive $\gamma\gamma$ sample, but requiring one of the photons to have $t_\gamma > 25$ ns. Similarly, we create a beam halo-enhanced sample from events that were filtered out from our signal sample by the beam halo rejection requirements [17]. We estimate the noncollision background events in the signal region using extrapolation techniques and the measured efficiencies of the noncollision rejection requirements [15]. The uncertainties on both noncollision background estimates are dominated by the statistical uncertainty on the number of identified events. Figure 1 (top) shows the \cancel{E}_T -significance distribution for the inclusive $\gamma\gamma$ sample, along with the predictions for all the backgrounds.

We estimate the sensitivity to heavy, neutral particles that decay to photons using the GMSB reference model [6] in the mass-lifetime range, $75 \leq m_{\tilde{\chi}_1^0} \leq 150$ GeV and $\tau_{\tilde{\chi}_1^0} \leq 2$ ns. Events from all SUSY processes considered [21] are simulated with PYTHIA followed by a detector simulation. The fraction of $\tilde{\chi}_1^0$ decays that occur in the detector volume, and thus the acceptance, depend on both the lifetime and the masses of the sparticles [11]. The total systematic uncertainty on the acceptance, after all kinematic requirements (discussed below), is estimated to be 7%, dominated by the uncertainty in the photon identification efficiency (2.5% per photon). Other significant contributions come from uncertainties on ISR and FSR (4%), jet energy measurement (2%), \cancel{E}_T -significance parametrizations (1%) and parton distribution functions (PDFs, 1%).

We determine the final kinematic selection requirements by optimizing the mean expected 95% confidence level (C.L.) cross section limit using a no-signal assumption, before looking at the data in the signal region [22]. To compute the predicted cross section upper limit we combine the luminosity, the acceptance, and the background estimates with their systematic uncertainties using a Bayesian method [23]. The predicted limits are optimized by simultaneously varying the selection requirements for \cancel{E}_T significance, H_T (scalar sum of E_T of photons, jets, and \cancel{E}_T), and the azimuthal angle between the two leading photons, $\Delta\phi(\gamma_1, \gamma_2)$. The large \cancel{E}_T -significance requirement eliminates most of the SM background with fake \cancel{E}_T . GMSB production is dominated by heavy gaugino pairs which decay to high- E_T light final state particles via cascade decays. The GMSB signal has, on average, larger H_T compared to SM backgrounds so that an H_T requirement

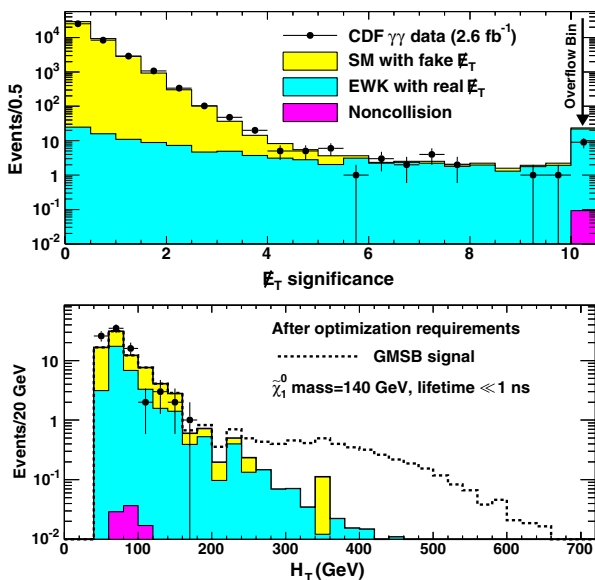


FIG. 1 (color online). The top plot shows the \cancel{E}_T -significance distribution for the inclusive $\gamma\gamma$ candidate sample, along with the background predictions. The bottom plot shows the predicted H_T distribution after all but the final H_T requirement.

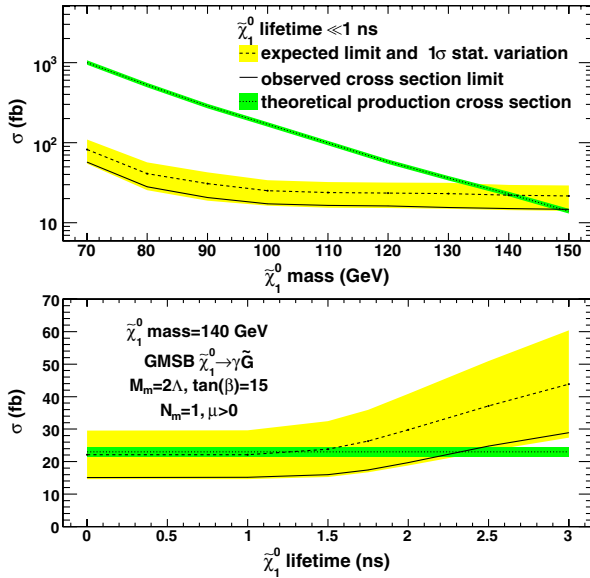


FIG. 2 (color online). The predicted and observed 95% C.L. cross section upper limits as a function of the $\tilde{\chi}_1^0$ mass at $\tau_{\tilde{\chi}_1^0} \ll 1$ ns (top) and as a function of the $\tilde{\chi}_1^0$ lifetime at $m_{\tilde{\chi}_1^0} = 140$ GeV/ c^2 (bottom). Indicated in green (darker shading) is the production cross section, along with its 8.0% uncertainty-band. In yellow (lighter shading) is the RMS variation on the expected cross section limit.

can remove these backgrounds effectively. Electroweak backgrounds with large H_T typically consist of a high- E_T photon recoiling against $W \rightarrow e\nu$, identified as $\gamma_{\text{fake}}\cancel{E}_T$, which means the gauge boson decay is highly boosted. Thus, the two photon candidates in the final state are mostly back to back. The SM backgrounds with fake \cancel{E}_T and large H_T also have photons which are mostly back to back; the $\Delta\phi(\gamma_1, \gamma_2)$ requirement, therefore, reduces both these backgrounds.

The optimal set of requirements is slightly different for each point in the $\tau_{\tilde{\chi}_1^0}$ vs $m_{\tilde{\chi}_1^0}$ space considered. We choose a single set of requirements to maximize the region where the predicted production cross section at next-to-leading order [24] is above the expected 95% C.L. cross section limit. The exclusion region also takes into account the production cross section uncertainties, which are dominated by the PDFs (7%) and the renormalization scale (3%). We find the optimal set of requirements, before unblinding the signal region, to be \cancel{E}_T significance > 3 , $H_T > 200$ GeV, and $\Delta\phi(\gamma_1, \gamma_2) < \pi - 0.35$. With these requirements we predict 1.4 ± 0.4 background events, 0.9 ± 0.4 of which are from electroweak sources (dominated by $Z\gamma\gamma$ production) with real \cancel{E}_T , 0.5 ± 0.2 from SM with fake \cancel{E}_T , and $0.001^{+0.008}_{-0.001}$ from noncollision sources. The acceptance for $m_{\tilde{\chi}_1^0} = 140$ GeV/ c^2 and $\tau_{\tilde{\chi}_1^0} \ll 1$ ns is estimated to be $7.8 \pm 0.6\%$.

No events in the data pass the final event selection. The predicted H_T distribution is shown in Fig. 1 (bottom), after

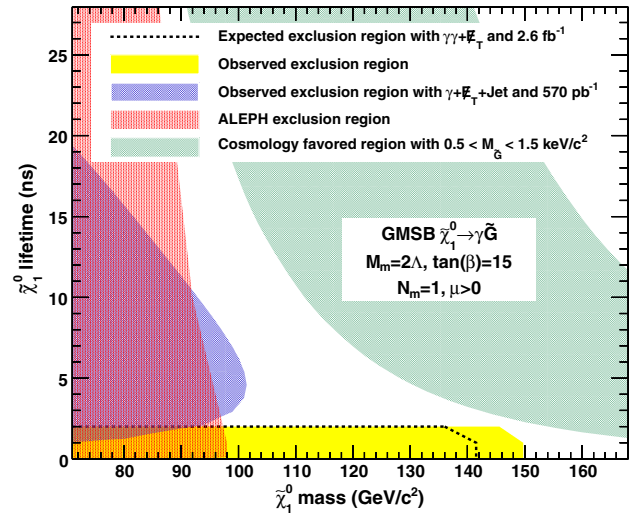


FIG. 3 (color online). The predicted and observed exclusion region along with the limits found in [10,17]. The shaded band shows the parameter space where $0.5 < m_{\tilde{G}} < 1.5$ keV/ c^2 , favored by cosmological models [7].

all but the final H_T requirement. The data are consistent with the no-signal hypothesis and are well modeled by SM backgrounds alone. We set cross section limits as a function of $m_{\tilde{\chi}_1^0}$ and $\tau_{\tilde{\chi}_1^0}$, respectively, as shown in Fig. 2. The $m_{\tilde{\chi}_1^0}$ reach, based on the predicted and observed number of events for $\tau_{\tilde{\chi}_1^0} \ll 1$ ns, is 141 GeV/ c^2 and 149 GeV/ c^2 respectively. These limits significantly extend the search sensitivity beyond the results of the D0 Collaboration [9], expand the results to include exclusions for $\tau_{\tilde{\chi}_1^0} \leq 2$ ns, and, when combined with the complementary limits from CDF and LEP [10,17], cover the region shown in Fig. 3.

In conclusion, we have performed an optimized search for heavy, neutral particles that decay to photons in the $\gamma\gamma + \cancel{E}_T$ final state using 2.6 ± 0.2 fb $^{-1}$ of data. There is no excess of events beyond expectations. We set cross section limits using a GMSB model with $\tilde{\chi}_1^0 \rightarrow \gamma\tilde{G}$, and find an exclusion region in the $\tau_{\tilde{\chi}_1^0} - m_{\tilde{\chi}_1^0}$ plane with the world's best 95% C.L. lower limit on the $\tilde{\chi}_1^0$ mass of 149 GeV/ c^2 at $\tau_{\tilde{\chi}_1^0} \ll 1$ ns. By the end of Run II, with an integrated luminosity of 10 fb $^{-1}$, we estimate a mass reach of ≈ 160 GeV/ c^2 .

We thank the Fermilab staff and the technical staffs of the participating institutions for their vital contributions. This work was supported by the U.S. Department of Energy and National Science Foundation; the Italian Istituto Nazionale di Fisica Nucleare; the Ministry of Education, Culture, Sports, Science and Technology of Japan; the Natural Sciences and Engineering Research Council of Canada; the National Science Council of the Republic of China; the Swiss National Science Foundation; the A. P. Sloan Foundation; the Bundesministerium für Bildung und Forschung, Germany; the World Class

University Program, the National Research Foundation of Korea; the Science and Technology Facilities Council and the Royal Society, U.K.; the Institut National de Physique Nucleaire et Physique des Particules, CNRS; the Russian Foundation for Basic Research; the Ministerio de Ciencia e Innovación, and Programa Consolider-Ingenio 2010, Spain; the Slovak R&D Agency; and the Academy of Finland.

^aDeceased.

^bVisitor from University of Massachusetts, Amherst, Amherst, MA 01003, USA.

^cVisitor from Universiteit Antwerpen, B-2610 Antwerp, Belgium.

^dVisitor from University of Bristol, Bristol BS8 1TL, United Kingdom.

^eVisitor from Chinese Academy of Sciences, Beijing 100864, China.

^fVisitor from Istituto Nazionale di Fisica Nucleare, Sezione di Cagliari, 09042 Monserrato (Cagliari), Italy.

^gVisitor from University of California Irvine, Irvine, CA 92697, USA.

^hVisitor from University of California Santa Cruz, Santa Cruz, CA 95064, USA.

ⁱVisitor from Cornell University, Ithaca, NY 14853, USA.

^jVisitor from University of Cyprus, Nicosia CY-1678, Cyprus.

^kVisitor from University College Dublin, Dublin 4, Ireland.

^lVisitor from University of Edinburgh, Edinburgh EH9 3JZ, United Kingdom.

^mVisitor from University of Fukui, Fukui City, Fukui Prefecture, Japan 910-0017.

ⁿVisitor from Kinki University, Higashi-Osaka City, Japan 577-8502.

^oVisitor from Universidad Iberoamericana, Mexico D.F., Mexico.

^pVisitor from University of Iowa, Iowa City, IA 52242, USA.

^qVisitor from Kansas State University, Manhattan, KS 66506, USA.

^rVisitor from Queen Mary, University of London, London, E1 4NS, United Kingdom.

^sVisitor from University of Manchester, Manchester M13 9PL, United Kingdom.

^tVisitor from Muons, Inc., Batavia, IL 60510, USA.

^uVisitor from Nagasaki Institute of Applied Science, Nagasaki, Japan.

^vVisitor from University of Notre Dame, Notre Dame, IN 46556, USA.

^wVisitor from University de Oviedo, E-33007 Oviedo, Spain.

^xVisitor from Texas Tech University, Lubbock, TX 79609, USA.

^yVisitor from IFIC(CSIC-Universitat de Valencia), 56071 Valencia, Spain.

^zVisitor from Universidad Tecnica Federico Santa Maria, 110v Valparaiso, Chile.

^{aa}Visitor from University of Virginia, Charlottesville, VA 22906, USA.

^{bb}Visitor from Bergische Universität Wuppertal, 42097 Wuppertal, Germany.

^{cc}Visitor from Yarmouk University, Irbid 211-63, Jordan.

^{dd}On leave from J. Stefan Institute, Ljubljana, Slovenia.

- [1] S. Dimopoulos, S. Thomas, and J. Wells, Nucl. Phys. **B488**, 39 (1997); S. Ambrosanio, G.D. Kribs, and S.P. Martin, Phys. Rev. D **56**, 1761 (1997); G. Giudice and R. Rattazzi, Phys. Rep. **322**, 419 (1999); S. Ambrosanio, G.L. Kane, G.D. Kribs, S.P. Martin, and S. Mrenna, Phys. Rev. D **55**, 1372 (1997).
- [2] We use a cylindrical coordinate system in which the proton beam travels along the z axis, θ is the polar angle, ϕ is the azimuthal angle relative to the horizontal plane, and $\eta = -\ln \tan(\theta/2)$. The transverse energy and momentum are defined as $E_T = E \sin\theta$ and $p_T = p \sin\theta$ where E is the energy measured by the calorimeter and p the momentum measured in the tracking system. $\cancel{E}_T = |\sum_i E_T^i \vec{n}_i|$ where \vec{n}_i is a unit vector that points from the interaction vertex to the i th calorimeter tower in the transverse plane.
- [3] F. Abe *et al.* (CDF Collaboration), Phys. Rev. Lett. **81**, 1791 (1998); Phys. Rev. D **59**, 092002 (1999).
- [4] S. Martin, arXiv:hep-ph/9709356.
- [5] P. Bode, J. Ostriker, and N. Turok, Astrophys. J. **556**, 93 (2001).
- [6] B. Allanach *et al.*, Eur. Phys. J. C **25**, 113 (2002). We use benchmark model 8 and take the messenger mass scale $M_m = 2\Lambda$, $\tan(\beta) = 15$, $\mu > 0$ and the number of messenger fields $N_m = 1$. The \tilde{G} mass factor and the supersymmetry breaking scale Λ are allowed to vary independently.
- [7] C.-H. Chen and J.F. Gunion, Phys. Rev. D **58**, 075005 (1998).
- [8] D. Acosta *et al.* (CDF Collaboration), Phys. Rev. D **71**, 031104 (2005).
- [9] V. Abazov *et al.* (D0 Collaboration), Phys. Lett. B **659**, 856 (2008).
- [10] R. Barate *et al.* (ALEPH Collaboration), Eur. Phys. J. C **28**, 1 (2003); also see M. Gataullin, S. Rosier, L. Xia, and H. Yang, arXiv:hep-ex/0611010; G. Abbiendi *et al.* (OPAL Collaboration), Proc. Sci. High Energy Phys. **2005** 346 (2006); J. Abdallah *et al.* (DELPHI Collaboration), Eur. Phys. J. C **38**, 395 (2005).
- [11] D. Toback and P. Wagner, Phys. Rev. D **70**, 114032 (2004).
- [12] E. Lee, Ph.D. thesis, Texas A&M University, 2010.
- [13] D. Acosta *et al.* (CDF Collaboration), Phys. Rev. D **71**, 032001 (2005).
- [14] M. Goncharov *et al.*, Nucl. Instrum. Methods Phys. Res., Sect. A **565**, 543 (2006).
- [15] T. Aaltonen *et al.* (CDF Collaboration), arXiv:0910.5170 [Phys. Rev. D (to be published)].
- [16] For a discussion of the jet energy measurements, see T. Affolder *et al.* (CDF Collaboration), Phys. Rev. D **64**, 032001 (2001); for a discussion of standard jet correction systematics, see A. Bhatti *et al.*, Nucl. Instrum. Methods

- Phys. Res., Sect. A **566**, 375 (2006). We use jets with cone size $\Delta R = 0.4$.
- [17] A. Abulencia *et al.* (CDF Collaboration), Phys. Rev. Lett. **99**, 121801 (2007); T. Aaltonen *et al.* (CDF Collaboration), Phys. Rev. D **78**, 032015 (2008).
- [18] T. Sjöstrand *et al.*, Comput. Phys. Commun. **135**, 238 (2001). We use version 6.216.
- [19] We use the standard GEANT-based detector simulation [R. Brun *et al.*, CERN-DD/EE/84-1, 1987] and add a parametrized EMTiming simulation.
- [20] U. Baur, T. Han, and J. Ohnemus, Phys. Rev. D **48**, 5140 (1993); U. Baur, T. Han, and J. Ohnemus, *ibid.* **57**, 2823 (1998); the $W\gamma$ and $Z\gamma$ processes are simulated using the leading-order event generator with a k factor fixed at 1.36. Initial and final state radiation (resulting in additional jets or photons), underlying event, and additional interactions are simulated using PYTHIA [18].
- [21] P. Simeon and D. Toback, J. Undergrad. Res. Phys. **20**, 1 (2007).
- [22] E. Boos, A. Vologdin, D. Toback, and J. Gaspard, Phys. Rev. D **66**, 013011 (2002).
- [23] T. Junk, Nucl. Instrum. Methods Phys. Res., Sect. A **434**, 435 (1999).
- [24] We use the leading-order cross sections generated by PYTHIA [18] and the k factors produced by PROSPINO 2.0 [W. Beenakker *et al.*, Phys. Rev. Lett. **83**, 3780 (1999)].